Current Eye Research

ISSN: 0271-3683 (Print) 1460-2202 (Online) Journal homepage: http://www.tandfonline.com/loi/icey20

Characterizing the Retinal Function of Psammomys obesus: A Diurnal Rodent Model to Study Human Retinal Function

Ahmed Dellaa, Anna Polosa, Sihem Mbarek, Imane Hammoum, Riadh Messaoud, Soumaya Amara, Rached Azaiz, Ridha Charfeddine, Mohamed Dogui, Moncef Khairallah, Pierre Lachapelle & Rafika Ben Chaouacha-Chekir

To cite this article: Ahmed Dellaa, Anna Polosa, Sihem Mbarek, Imane Hammoum, Riadh Messaoud, Soumaya Amara, Rached Azaiz, Ridha Charfeddine, Mohamed Dogui, Moncef Khairallah, Pierre Lachapelle & Rafika Ben Chaouacha-Chekir (2016): Characterizing the Retinal Function of Psammomys obesus: A Diurnal Rodent Model to Study Human Retinal Function, Current Eye Research, DOI: 10.3109/02713683.2016.1141963

To link to this article: http://dx.doi.org/10.3109/02713683.2016.1141963

Published online: 23 May 2016.

CURRENT EYE RESEARCH
http://dx.doi.org/10.3109/02713683.2016.1141963

Taylor & Francis
Taylor & Francis Group

Characterizing the Retinal Function of *Psammomys obesus*: A Diurnal Rodent Model to Study Human Retinal Function

Ahmed Dellaa [a,b], Anna Polosa[c], Sihem Mbarek[a], Imane Hammoum[a], Riadh Messaoud[d], Soumaya Amara[d], Rached Azaiz[e], Ridha Charfeddine[e], Mohamed Dogui[f], Moncef Khairallah[d], Pierre Lachapelle[c], and Rafika Ben Chaouacha-Chekir[a]

[a]UR Ecophysiologie et Procédés Agroalimentaires, Institut Supérieur de Biotechnologie, Université de la Manouba, Ariana, Tunisie; [b]Faculté des Sciences de Bizerte, Université de Carthage, Zarzouna, Tunisia; [c]Département d'Ophtalmologie, Institut de Recherche du Centre Universitaire de santé McGill, Montréal, Canada; [d]Service d'Ophtalmologie, CHU Fattouma Bourguiba, Monastir, Tunisie; [e]Industrie Pharmaceutique UNIMED, Zone Industrielle, Kalaa Kebira, Sousse, Tunisie; [f]Service d'Explorations Fonctionnelles du Système Nerveux, Hôpital Universitaire Sahloul, Sousse, Tunisie

ABSTRACT

Purpose: To compare the retinal function of a diurnal murid rodent, *Psammomys obesus*, with that of Wistar albino rat and human subjects.

Materials and methods: Adult *Psammomys obesus* were captured and transferred to the animal facilities where they were maintained at 25°C with standard light/dark cycles and natural halophilic plants, rich in water and mineral salts. Standard full-field photopic and scotopic electroretinograms were obtained.

Results: The right eye of all animals displayed well detectable and reproducible scotopic and photopic electroretinogram (ERG) responses. Results were compared with those obtained from human subjects and Wistar rats. ERG measurement showed that the amplitudes of scotopic responses in *Psammomys obesus* are quite similar to those of human subjects. The amplitude of the photopic a-wave was comparable to that of humans and six times higher than that of the albino rat. The amplitudes of photopic b-wave, photopic oscillatory potentials (OPs), and 30 Hz flicker were all markedly larger in *Psammomys obesus* compared to those obtained from human subjects and Wistar rats. Furthermore, like the human photopic ERG, the photopic ERG of *Psammomys obesus* also includes prominent post b-wave components (i.e. i- and d-waves) while the ERG of Wistar rats does not.

Conclusions: Our results suggest that the retinal function of *Psammomys obesus*, especially the cone-mediated function, shares several features with that of human subjects. We believe that *Psammomys obesus* represents an interesting alternative to study the structure and function of the normal and diseased retina in a human-like rodent model of retinal function.

ARTICLE HISTORY
Received 22 June 2015
Revised 15 December 2015
Accepted 5 January 2016

KEYWORDS
Cone; diurnal; electroretinogram; oscillatory potential; *Psammomys obesus*

Introduction

Psammomys obesus (P.obesus), a herbivorous rodent, has become an important animal model of the nutritionally induced type-2 diabetes used in biological and medical research.[1–3] The retina of *P.obesus* contains a high proportion of cone, which is estimated to be at approximately 41% of the total photoreceptors.[4] Several neuronal and vascular anomalies, similar to those found in human diabetic retinopathy (DR), have also been identified in *P.obesus*.[5,6] While several rodent models of DR exist, with varying degrees of similarity to the human disease,[7] some structural and molecular changes observed in *P.obesus* and human retinas have not been observed in other animal models, attesting to the value of using this animal model in translational research.[5]

It is well documented that the retinal function, as assessed with the electroretinogram,[8] is impaired (especially the oscillatory potentials, OPs) in patients affected with diabetes, and that, often long before the appearance of clinical signs at fundus examination.[7] The OPs are known to be a highly sensitive diagnostic tool to detect and follow-up disease progression of retinal degeneration, such as DR.[9–11] Given the similarities shared between the retinal structure of *P. obesus* and human subjects and the fact that *P.obesus* also represents a valid animal model of human type-2 diabetes, the purpose of this study was to characterize the retinal function of *P.obesus* to determine if it could represent a better animal model of human retinal function compared to the more widely used albino Sprague Dawley albino rats.

Materials and methods

Animals

Psammomys obesus are common in North Africa and were captured in a semi-desertic area of southern Tunisia (near the Bouhedma national park) in strict accordance with the national regulations on the treatment of wildlife. Following capture, each *P.obesus* specimen was examined by a veterinarian, found healthy, and subsequently held in quarantine for adaptation prior to experimentation. This study was performed on 12 adult males *P.obesus* (mean weight 120 g;

CONTACT Rafika Ben Chaouacha-Chekir raf_chekir@yahoo.fr UR Ecophysiologie et Procédés Agroalimentaires, Institut Supérieur de Biotechnologie, Université de la Manouba, Sidi Thabet 2020 Ariana, Tunisie.

range 100–140 g). Data was compared to that obtained from Wistar rats (n = 6: adult males from a total of 10 animals used at the beginning in ERG measuring) and human (n = 6: adult males 20–28 years). During the study, *P.obesus* and Wistar rats were maintained on 12 h light/dark cycle (light ~ 30 cd/m^2), with free access to food and water. *P.obesus* received a natural hypocaloric (0.4 kcal/g wet weight) vegetable diet, i.e., halophilic plants (chenopodiaceae), rich in water and mineral salts, whereas Wistar rats received a standard diet. All treatments were in compliance with both standards for wildlife and standards for laboratory animals. The room temperature was 24°C and the relative humidity varied between 65 and 70%. Animals were used and handled according to the principles of the ARVO statement for the use of animals in ophthalmic and vision research.

ERG recording

Following overnight dark adaptation, animals were prepared for ERG recording under a dim red light. All ERGs were collected between 9 and 15 h. After an anesthesia with ketamine (120 mg/kg), the pupil of the right eye was dilated with drops of Tropicamide (25 mg/5 ml; UNIMED, Tunisia) and the animal was laid on its left side on a homoeothermic blanket set at 38°C. A modified contact lens electrode (ERG-Jet Lens, Fabrinalsa, Sweden) lubricated with ophthalmic gel (Lacryvisc, Carbomer 974 P, Alcon), to prevent dehydration and to ensure optimal electrical contact, was used. The reference and ground electrodes were inserted subcutaneously on the forehead and tail, respectively. The Vision Monitor system (Metrovision, France) provided stimulus presentation and data acquisition. The five different basic ERG responses advocated by the International Society for Clinical Electrophysiology of Vision[12] were used to compare the retinal function of the three groups.

The scotopic ERG responses (Amplification: x 12500; 1–1200 Hz bandwidth) were evoked to flashes of white light of 0.01 cd.s/m^2 (rod responses) and 3cd.s/m^2 (mix rod-cone response and OPs). The OPs were extracted from ERG signal by Fourier transform using an 80–200 Hz bandwidth. Photopic ERG responses were obtained after the scotopic responses following a 10-minute period of light adaptation to a background of 30 cd.m^{-2}. Photopic ERGs (average, 20 flashes, interstimulus interval: 1 second) were evoked to a 3cd.s/m^2 flash presented against a rod desensitizing background of 30 cd/m^2. A 30 Hz flicker response was also obtained using the same flash intensity and background luminance.

Finally, photopic OFF response was recorded using a flash of 312 ms in duration, which was delivered against a photopic background light of 30 cd.s/m^2 in luminance.

Human subject

The ERG responses of human subjects were collected using the same protocol and recording system described above except for the dark adaptation period, which only lasted 20 minutes as recommended by the ISCEV standard.[12]

Data analysis

Responses were analyzed as suggested by the ISCEV standard. The amplitude of the a-wave was calculated from the baseline to the first negative deflection, and the amplitude of the b-wave was measured from the trough of the a-wave to the positive peak of the b-wave. We also measured the amplitude of the i-wave from the trough of the b-wave to the peak of the i-wave. The amplitudes of the OPs were estimated by measuring the heights from the baseline drawn between the troughs of successive wavelets to their peaks. The OPs were extracted digitally by using the Metrovision software. The amplitude of the flicker ERG was measured from the trough to the peak. The peak time was measured from stimulus onset to the corresponding peak.[12,13] For all data presented, the values on the graph represent the mean ± SEM. Statistical comparisons between the results obtained from the different species were performed with multiple comparison one-way ANOVA. T-test was used to compare two groups. *P* values less than 0.05 were considered significant. All values are presented as mean ± SEM.

Results

As evidenced from Figure 1, the scotopic ERGs of all three species are comparable in amplitude, peak time, and morphology. Response differences were more pronounced with the photopic ERG signal, which differed not only in amplitude, but also in morphology and peak time. Of note, like in human photopic ERG response, the b-wave of *P.obesus* was also followed by another positive wave (the i-wave), while, as previously shown,[14] the photopic ERG of Wistar rats does not include a visible i-wave. All individual values were illustrated as scatter and box plots (Figures 2 and 3).

Scotopic conditions

Figure 1A shows the scotopic ERG evoked at an intensity of 0.01 cd s/m^2. Amplitude and peak time measurements are reported at Table 1. We notice that the amplitude of the scotopic b-wave of *P.obesus* (339.75 ± 16.52 μV) is quite similar to that measured in human subjects (309.18 ± 12.96 μV) compared to that of Wistar rats (403.25 ± 15.26 μV), which is the largest (rat vs. *P.obesus:* $p < 0.05$; rat vs. human: $p < 0.01$). In contrast, no significant amplitude differences were noted with the mix rod-cone b-wave (Figure 1B) as seen in Table 1 (*P.obesus*, human, and rat: 492.33 ± 22.26 μV, 454.33 ± 20.76 μV, and 542.66 ± 13.71 μV, respectively; $p > 0.05$) while the amplitude of the a-wave measured in human ERGs (218 ± 17 μV) is significantly larger than that of *P.obesus* (181.91 ± 10.53 μV, $p < 0.05$) and close to that of the rat ERG (201.83 ± 9.9 μV).

Moreover, we also examined the b/a ratio (Figure 4) at 3 cd s/m^2, which is an index to compare the synaptic transmission from the photoreceptor to the inner retina.[16,17] In scotopic condition, similar b/a ratios were obtained from all three species (*P.obesus*, human, and rat: 2.79 ± 0.17, 2.05 ± 0.14, 2.7 ± 0.13 respectively; $p > 0.05$).

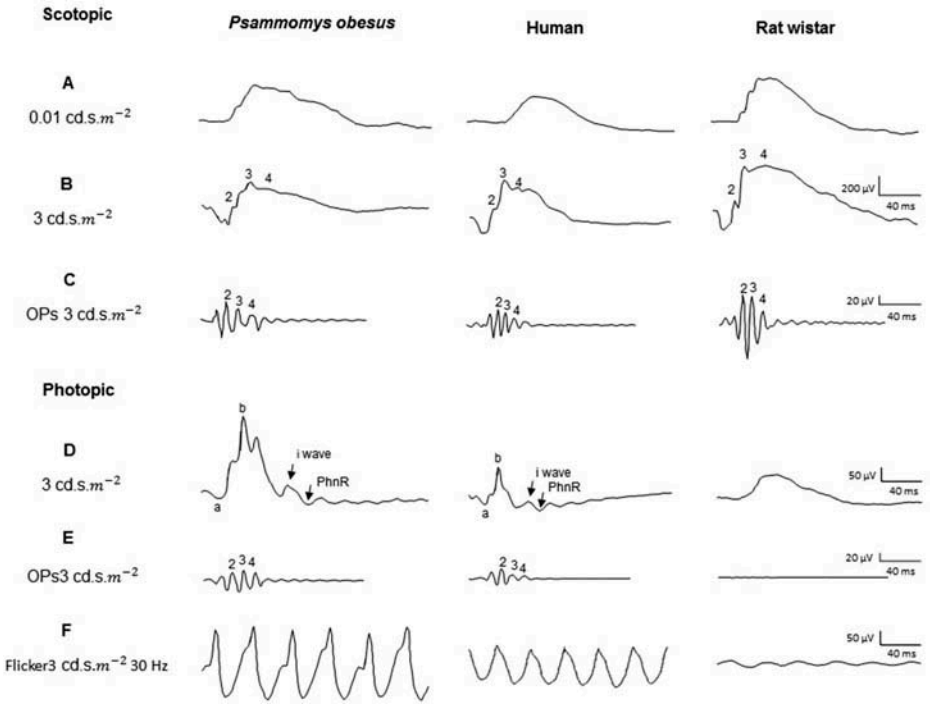

Figure 1. Standard responses for full-field electroretinography in *Psammomys obesus*, human, and Wistar rat, including a typical electroretinographical curves response: a rod-driven response, a combined rod–cone response, oscillatory potentials, a cone response, and a flicker response. (A) Rod response stimulated using 0.01 cd.s/m^2 light intensities stimulation under scotopic condition. (B) Mixed response elicited at 3 cd.s/m^2 in the dark adapted eye. (C) Oscillatory potentials elicited in the scotopic condition. (D) Photopic cone response at 3 cd.s/m^2 after 10 minutes of light adaptation with 30 cd/m^2 background. (E) Photopic oscillatory potential extracted from 3 cd.s/m^2 cone response. (F) Flicker 30 Hz response: (a) a-wave, (b) b-wave, (i) i-wave, (PhnR) photopic negative response, (2) OP2, (3) OP3, (4) OP4. Horizontal calibration: 40 ms. Vertical calibration: 200 µV (scotopic ERG); 100 µV (photopic ERG); 20 µV (OPs).

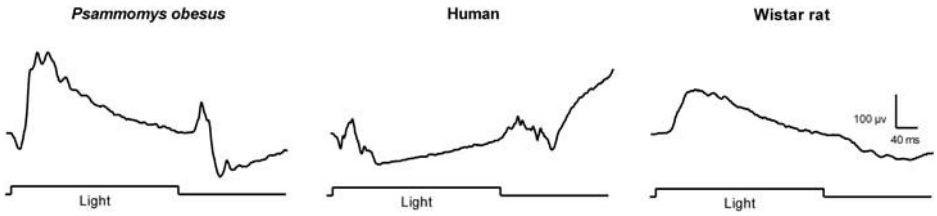

Figure 2. Values of the scotopic and photopic ERG amplitude and peak time between *Psammomys obesus* (P), human (H), and Wistar rat (W). **(A, B)** Scatter plot representation for ERG amplitude and peak time. **(C, D)** Box plot representation for ERG amplitude and peak time.

As for the temporal parameters (Table 1), the peak time of the dim flash rod b-wave (0.01 cd s/m^2 stimulus) of *P.obesus* ERG (54.17 ± 1.69 ms) was similar to that of the Wistar rat (56.3 ± 3.96 ms; $p > 0.05$) and significantly faster than that of human subjects (77.05 ± 2.35 ms, $p < 0.001$). However in the mix rod-cone ERG, the peak time of the b-wave of *P.obesus* ERG (47.00 ± 1.32 ms) is similar to that of human (45.17 ± 2.18 ms) and significantly faster than that of the Wistar rat (35.22 ± 1.76 ms, $p < 0.001$). Similarly, the peak time of the mix rod-cone a-wave of *P.obesus* (17.86 ± 0.71 ms) was similar to that of human (20.57 ± 1.96 ms), but significantly faster in rats (12.82 ± 1.38 ms, $p < 0.01$).

Faster components of lower amplitude, known as the OPs, are seen on the ascending limb of the scotopic b-wave (Figure 1C). Table 2 shows the amplitudes and peak time of individual OPs (OP2, OP3, and OP4) in scotopic condition measured for the three species.

The sum amplitudes of the scotopic OPs in *P.obesus* (164.94 ± 12.08 µV) are quite close to those of humans (143.89 ± 12.64 µV), while significantly larger OPs were measured in the ERG of Wistar rat (284.98 ± 35.35 µV; *P. obesus* vs. rat: $p < 0.01$; human vs. rat: $p < 0.001$).

The data given in Table 2 indicates that there is no significant difference measured in OP2 amplitude among *P.obesus*, human, and rat (74.04 ± 7.71 µV, 61.43 ± 5.08 µV, and 98.73 ± 16.84 µV, respectively). However, a significant peak time difference was noted between human and rat ($p < 0.01$). Similarly, while the amplitude of OP3 was similar in *P.obesus* (49.28 ± 4.67 µV) and human (45.40 ± 4.99 µV), it was significantly lower than the ERG of Wistar rats (104, 30 ± 20.33 µV). Finally, while no significant OP4 amplitude difference was noted between *P.obesus* (41.62 ± 6.31 µV) and human (37.06 ± 4.58 µV), a significantly larger amplitude was noted in rat (61.85 ± 8.71 µV; $p < 0.05$). There is also a significant time difference measured for OP3 and OP4 such that the OP2–OP3 and OP3–OP4 interpeak intervals were significantly longer in *P.obesus* and

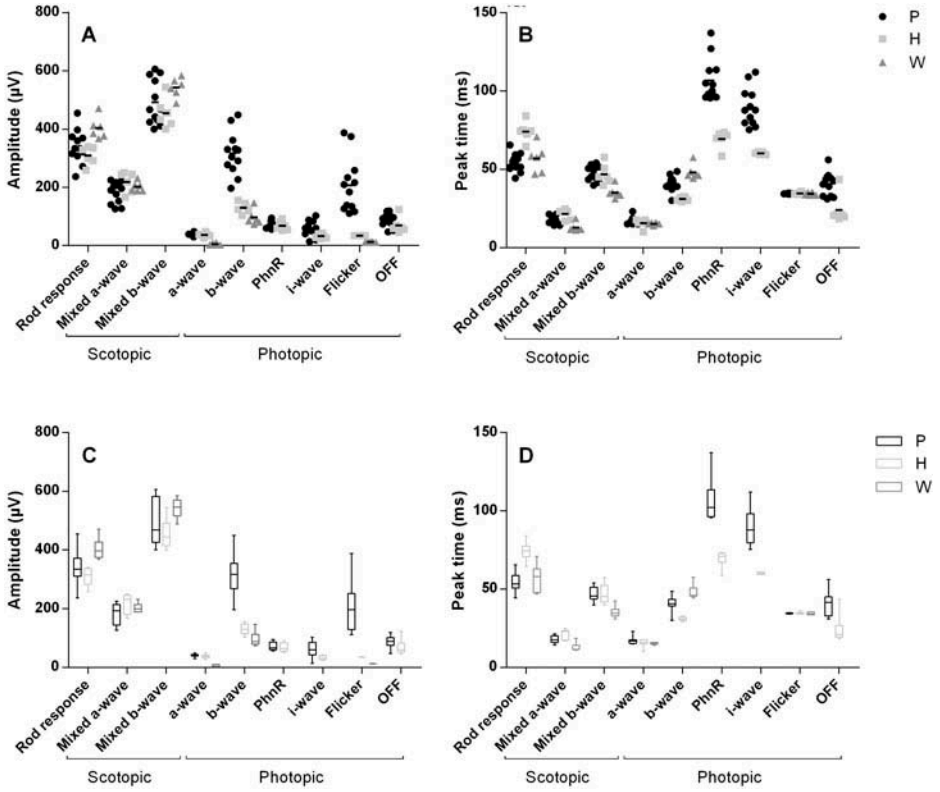

Figure 3. Values of the OPs amplitudes and peak times between *Psammomys obesus* (P), human (H), and Wistar rat (W). **(A, B)** Scatter plot representation for ERG amplitude and peak time. **(C, D)** Box plot representation for ERG amplitude and peak time.

Table 1. Comparison of ERG recordings values of the amplitude (μV) and implicit time (ms) between *Psammomys obesus*, human, and Wistar rat.

Adaptation status	Responses (Amplitude: μV)	*Psammomys obesus*	Human	Wistar Rat
Dark	Rod response	339.75 ± 16.52†	309.18 ± 12.96$^{\#\#}$	403.25 ± 15.26
	Mixed a-wave	181.91 ± 10.53*	218 ± 17	201.83 ± 9.9
	Mixed b-wave	492.33 ± 22.26	454.33 ± 20.76	542.66 ± 13.71
Light	a-wave	32.81 ± 2.63†††	37.20 ± 2.90$^{\#\#\#}$	5.54 ± 1.87
	b-wave	316.13 ± 21.41***,†††	135.58 ± 6.00	90.94 ± 5.53
	PhnR	71.89 ± 4.03	67.64 ± 7.2	NA
	i-wave	60 ± 8.25*	32.5 ± 3.07	NA
	Flicker	207.52 ± 27.29*,†††	113.95 ± 18.20$^{\#}$	12.26 ± 0.36
	OFF response	88.5 ± 7.03	69.10 ± 7.97	NA
	Peak time (ms)			
Dark	Rod response	54.17 ± 1.69***	77.05 ± 2.35$^{\#\#\#}$	56.3 ± 3.96
	Mixed a-wave	17.86 ± 0.71††	20.57 ± 1.96$^{\#\#\#}$	12.82 ± 1.38
	Mixed b-wave	47.00 ± 1.32†††	45.17 ± 2.18$^{\#\#}$	35.22 ± 1.76
Light	a-wave	17.04 ± 0.63†	16.83 ± 0.75	21.38 ± 1.34
	b-wave	40.85 ± 1.39**††	31.6 ± 0.68$^{\#\#}$	47.98 ± 2.42
	PhnR	106.84 ± 3.88**	69.33 ± 2.26	NA
	i-wave	89.74 ± 3.67**	60.2 ± 0.32	NA
	Flicker	34.54 ± 0.08†††	34.52 ± 0.43$^{\#\#\#}$	17.5 ± 1.03
	OFF response	40.45 ± 2.35***	24.05 ± 2.7	NA

NA: not applicable

Data for *Psammomys obesus* (n = 12), human (n = 6), and Wistar rat (n = 6) were generated in this study. Values are reported as mean ± SEM. Statistical significance was tested with one-way ANOVA (Tukey Multiple comparison test).

*; †; #: $p < 0, 05$

**; ††; # #: $p < 0, 01$

***; †††; ###: $p < 0{,}001$

*: *P.obesus* vs. Human; †: *P.obesus* vs. Wistar rat; #: Human vs. Wistar rat.

Wistar rat than in human. Finally, despite the above-mentioned differences, the morphology of the scotopic ERG and OPs recorded from *P.obesus* and human subjects is strikingly similar and quite different from those recorded from the Wistar rats.

Photopic conditions

Under light adaptation, the a- and b-waves reflect cones-driven responses and these are typically smaller than responses recorded under scotopic conditions (Figure 1B and D). The a-wave amplitude for *P.obesus* (32.81 ± 2.63

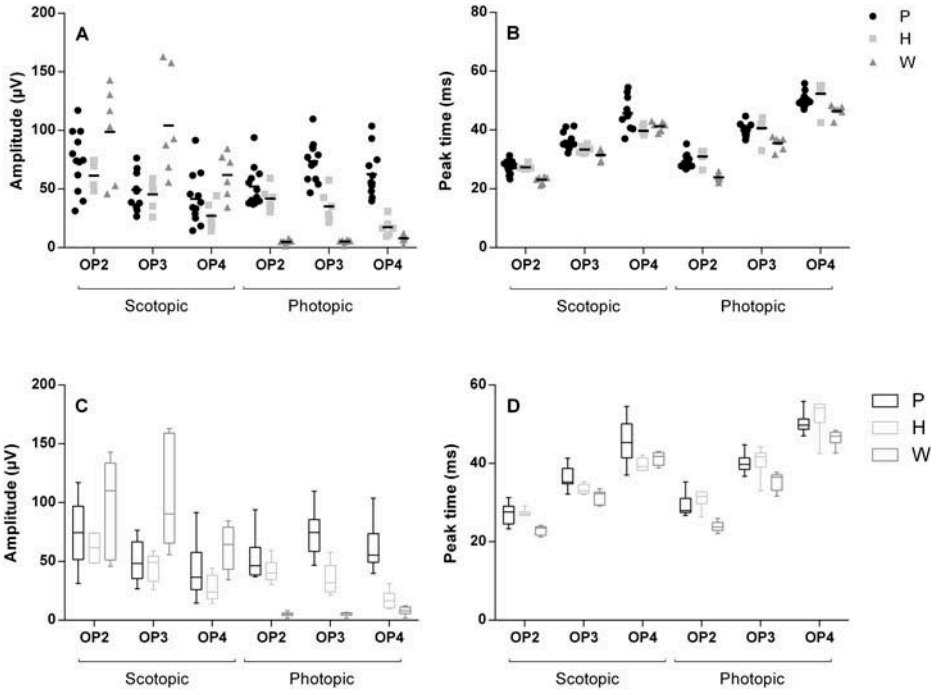

Figure 4. Comparison of values of the ratio of b-wave and a-wave amplitudes between *Psammomys obesus*, human, and Wistar rat. Data were obtained at a light intensity of 3 cd s/m2 in both scotopic and photopic conditions, the significance levels are given by asterisks as follows: *$p \leq 0.05$, ** $p \leq 0.01$, and *** $p \leq 0.001$.

μV) was similar to that of human (37.20 ± 2.90 μV), and six times smaller in Wistar rats (5.54 ± 1.87 μV). Similarly, the amplitude of the b-wave in *P.obesus* (316.13 ± 21.41 μV) was significantly larger than human (135.58 ± 6.00 μV) and rat (90.94 ± 5.53 μV). As expected from the results presented above, the amplitudes of photopic flicker responses in *P.obesus* (207.52 ± 27.29 μV) were also significantly larger than those of human (113.95 ± 18.2 μV) and Wistar rats (12.26 ± 0.23 μV). No significant differences were observed in the peak time of photopic flicker responses in *P.obesus* compared to human (Table 1). Similar to the human photopic ERG response, the ERG of *P.obesus* also included an easily identifiable i-wave, while the ERG of Wistar rats was devoid of this post-b-wave deflection. Of interest, the i-wave of *P.obesus's* ERG (arrowhead in Figure 1D) is almost twice the amplitude in human (60 ± 85.25 μV vs. 32.5 ± 3.07 μV; $p < 0.05$). Similarly, while the photopic negative response (PhNR) appears to be missing from the ERG of Wistar rats, it is easily identifiable and of similar amplitude in the ERGs of *P.obesus* and human subjects (71.89 ± 4.03 μV vs. 67.64 ± 7.27 μV; $p > 0.05$). The same goes for the OFF response (Figure 5), which was also absent from the recordings of Wistar rats while being the most prominent in *P.obesus* compared to human subjects (88.5 ± 7.03 μV vs. 69.10 ± 7.97 μV; $p < 0.05$). In photopic condition, the b/a ratio (Figure 4) measured for *P.obesus* (10.15 ± 0.84) is significantly lower than that of Wistar rats (27.49 ± 8.35) and significantly higher than that of human (3.53 ± 0.13).

Finally, as shown in Figure 1 (panel E) the photopic OPs were of significantly higher amplitude in *P.obesus* (188.38 ± 14.14 μV) compared to those in human (94.33 ± 7.84 μV) and Wistar rat (17.94 ± 2.62 μV). This amplitude difference between *P.obesus* and human was the most pronounced with OP3 and OP4 (Table 2). As exemplified in Table 2, the OP peak times were similar between *P.obesus* and slightly faster for Wistar rat. The latter had however no significant impact on the OP interpeak interval, which was similar for all species.

Discussion

In this paper, we present novel ERG data, which suggests that ERG of *Psammomys obesus*, especially the photopic ERG, shares several features with that of human subjects, making it an interesting alternative to study the structure and function of the normal and diseased retina in a human-like rodent model of retinal function. The amplitude of the photopic a-wave of *P.obesus* is close to that measured in human and higher than those obtained in rats and mice as well as those recorded from pure-cone transgenic mice, indicating strong, cone-driven, retinal responses.[15] Large a-wave amplitudes, similar to those of *P.obesus*, were also reported for the diurnal Nile grass rat whose retina contains more than 35% of cones[16] as well as the Mongolian gerbil with 13% of cones photoreceptors.[17] This result can be explained by the closure of cGMP-dependent Na+ channels leading probably to larger changes in the corneal potential in *P.obesus* than in rats and mice. Among other factors likely to contribute to larger light-driven changes in corneal potential are a higher number of cone and an elevated total surface area of cone. Estimates based on structural retina investigations show that *P.obesus*[4] retina has a considerably higher number of cones compared with rats and mice.[18–20] This cornea-negative component reflects mainly light-induced electrical activity in the photoreceptor.

Table 2. Normative data of oscillatory potentials for *Psammomys obesus*, human, and Wistar rat.

	OP2		OP3		OP4		Sum OPs	Intervals (ms)	
	Amplitude (µv)	Peak-time (ms)	Amplitude (µv)	Peak-time (ms)	Amplitude (µv)	Peak-time (ms)	Amplitude (µv)	OP2–OP3	OP3–OP4
Scotopic									
P.obesus	74.04 ± 7.41	26.97 ± 0.73††	49.28 ± 4.67†††	36.29 ± 0.83††	41.62 ± 6.31†	45.69 ± 1.49†	164.94 ± 12.08††	9.33 ± 0.78†††	9.39 ± 1.16†
Human	61.43 ± 5.08	27.31 ± 0.37$^{\#\#}$	45,40 ± 4,99$^{\#\#}$	33,36 ± 0,54	37.06 ± 4.58$^{\#}$	39.71 ± 0.65	143,89 ± 12.64$^{\#\#\#}$	6.05 ± 0.45$^{\#}$	6.35 ± 0.59$^{\#}$
Wistar rat	98.73 ± 16.84	23.01 ± 0.54	104.30 ± 20.33	31.50 ± 0.79	61.85 ± 8.71	41.30 ± 0,75	284.89 ± 35.35	8.49 ± 0.67	9.80 ± 0.77
Photopic									
P.obesus	52.11 ± 6.03†††	29.28 ± 0.89†††	73.70 ± 6.22***,†††	39.99 ± 0.76††	62.57 ± 6.93***,†††	50.37 ± 0.85	188.38 ± 14.14***,†††	10.71 ± 0.83	10,38 ± 0.80
Human	41.83 ± 4.12$^{\#\#\#}$	30,97 ± 0.97$^{\#\#\#}$	35.02 ± 5.49$^{\#\#}$	40.65 ± 1.59$^{\#\#}$	17.48 ± 3.12	52.34 ± 2.00$^{\#\#}$	94.33 ± 7.84$^{\#\#}$	9.69 ± 1.28	11,69 ± 1.79
Wistar rat	4.98 ± 0.83	23.90 ± 0.53	5.11 ± 0.71	35.47 ± 0.95	7.86 ± 1.48	46.48 ± 0.83	17.94 ± 2.62	11.57 ± 0.74	11.01 ± 0.89

Summary amplitudes (µV) (Psammomys n = 12; Human n = 6; Wistar rat n = 6) and peak time (ms) of oscillatory potentials. Values are reported as mean ± SEM. Statistical significance was tested with one-way ANOVA (Tukey Multiple comparison test).

*; †; #: $p < 0, 05$

**; ††; # #: $p < 0, 01$

***; †††; ###: $p < 0{,}001$

*: *P.obesus* vs. Human; †: *P.obesus* vs. Wistar rat; #: Human vs. Wistar rat.

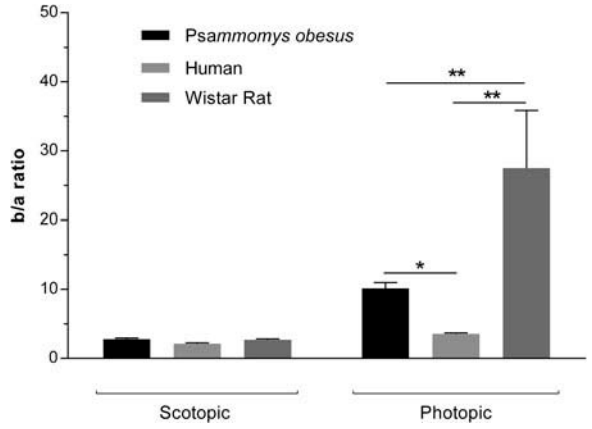

Figure 5. Representative traces of photopic OFF responses to long flash duration (312 ms) elicited at 2.36 log cd.s/m^2. Horizontal calibration: 40 ms. Vertical calibration: 50 μV. Solid line below trace illustrates light stimulus.

Furthermore, the lower ratio of photopic b-/a-wave amplitude in *P.obesus* compared with Wistar rats is another discrepancy from nocturnal rodents. This lower ratio is closer to the values recorded in human. Lower b/a values for cone-driven responses recorded under photopic and dark-adapted conditions reflect a higher proportion of a-wave contribution to the ERG response, implying cone hyperpolarization. The b/a ratio is significantly lower for *P.obesus* than for rat under photopic adapted conditions. The functional characterizing ERG studies in diurnal rodents, e.g. Nile grass rat16 and Mongolian Gerbil17, shows that the lower b/a ratio indicates that these animals have better synaptic transmission from cone to cone bipolar cells for amplification and bigger b-wave. Moreover, it had been reported that the b/a ratio can be used as a measure of the degree of retinal ischemia in central retinal vein obstruction.[21]

OPs, which are superimposed on the ERG b-wave (attributed to ON bipolar cell responses), are said to reflect synaptic activity within the inner retinal layers.[22] OP amplitude is an important parameter in assessing the function of the inner retina of the healthy and diseased retinas.[23,24] Many studies suggest that OPs reflect the activity of multiple generators[25–27] while others suggest that they are most probably generated by a single source.[28,29] Abnormalities in the OPs are of great interest in the assessment of DR where they have been reported to be reduced in amplitude[10,30–32] and delayed in timing.[33,34] By measuring the sum of OPs, we found that the photopic OPs of *P.obesus* were of higher amplitudes compared to human subjects and rats. *P.obesus* would therefore represent an interesting animal model to further investigate the origin of the OPs and to predict the development of proliferative DR.

The presence of a well-identifiable i-wave is another photopic ERG feature that *P.obesus* and human subjects share. This positive, post-b-wave, deflection is believed to represent the activity of ganglion cells and /or optic nerve.[35,36] It was previously shown to be present in the photopic ERGs of several other diurnal species like monkey, guinea pig, dog, rabbit, and mini-pig, but not in rats and mice.[14] The PhNR is another post-b-wave component that human and *P.obesus* shared. Several lines of evidence indicate that the PhNR originates from the spiking activity of the retinal ganglion cells and their axons in human and primates,[37–39] but in animals such as rodent its origin is controversial.[28,40–42] Previous studies have indicated that the PhNR may also be useful in the evaluation of retinal function for patients with retinal ischemic disorders, such as DR or central retinal vein occlusion.[37,43] Thus, the *P. obesus* model might offer complementary information to further study the physiological basis of the PhNR in rodents.

The results from white flicker 30 Hz stimuli on a 30 cd/m2 luminosity background indicate that *P.obesus* has a significantly higher flicker fusion than Wistar rat and human. Light-adapted flicker responses include cone photoreceptors, depolarizing bipolar cells,[44,45] and hyperpolarizing bipolar cells. The fast-flicker ERG is used to examine inner retina (cone-driven response) because rod-driven responses generally do not respond to fast flicker.[46] The ERG amplitude of *P.obesus* at 30Hz is much higher than that of rodent[47,48] and similar to the cone flicker of monkey[49] and human.[50]

In addition, similarity with human ERG[51] is that photopic OFF responses (d-wave) are larger in *P.obesus* than in Wistar rat and mice.[16] The d-wave is generated from OFF-cone pathway such as the OFF bipolar cells.[52,53] Our results indicate that OFF-cone circuity is more similar to human than nocturnal rodent.

Our findings indicate that cone-driven processing in the inner retina in *P.obesus* is physiologically closer to humans than rats.

The features of the present results recording in accordance with the ISCEV characterize diurnal mammal and are close to results obtained in human features. The difference with other rodents is especially in i-wave components, which generally are missing from photopic ERGs of rats. So as to provide a stable basis for comparison in future studies of pharmacology and disease, *P.obesus* promises to be a very interesting animal model for the exploration of disease affecting cone pathways. Moreover, genetic tools developed for the *Rattusgenus* are generally applicable to *P.obesus*.[4,6]

Acknowledgments

This study was supported by EU within the framework of PASRI program from The Ministry of Higher Education and Scientific Research in partnership with UNIMED Laboratories.

Declaration of interests

The authors report that they have no conflicts of interest. The authors alone are responsible for the content and writing of the paper.

ORCID

Ahmed Dellaa http://orcid.org/0000-0002-3685-7474

References

1. Gross DJ, Leibowitz G, Cerasi E, Kaiser N. Increased susceptibility of islets from diabetes-prone Psammomys obesus to the deleterious effects of chronic glucose exposure. Endocrinology 1996;137:5610–5615.
2. Kalman R, Adler J, Lazarovici G, Bar-On H, Ziv E. The efficiency of sand rat metabolism is responsible for development of obesity and

diabetes. Journal of basic and clinical physiology and pharmacology 1992;4:57–68.
3. Nesher R, Gross DJ, Donath MY, Cerasi E, Kaiser N. Interaction between genetic and dietary factors determines beta-cell function in Psammomys obesus, an animal model of type 2 diabetes. Diabetes. 1999;48:731–737.
4. Saidi T, Mbarek S, Chaouacha-Chekir RB, Hicks D. Diurnal rodents as animal models of human central vision: characterisation of the retina of the sand rat Psammomys obsesus. Graefes Arch Clin Exp Ophthalmol. 2011;249:1029–1037.
5. Saidi T, Chaouacha-Chekir R, Hicks D. Advantages of Psammomys obesus as an Animal Model to Study Diabetic Retinopathy. J Diabetes Metab 2012;3:2.
6. Saidi T, Mbarek S, Omri S, Behar-Cohen F, Chaouacha-Chekir RB, Hicks D. The sand rat, Psammomys obesus, develops type 2 diabetic retinopathy similar to humans. Invest Ophthalmol Vis Sci 2011;52:8993–9004.
7. Rees DA, Alcolado JC. Animal models of diabetes mellitus. Diabet Med 2005;22:359–370.
8. Steinberg RH, Linsenmeier RA, Griff ER. Chapter 2 Retinal pigment epithelial cell contributions to the electroretinogram and electrooculogram. Progress in Retinal Research 1985;4:33–66.
9. Bresnick GH, Korth K, Groo A, Palta M. Electroretinographic oscillatory potentials predict progression of diabetic retinopathy: preliminary report. Archives of ophthalmology 1984;102:1307–1311.
10. Vadala M, Anastasi M, Lodato G, Cillino S. Electroretinographic oscillatory potentials in insulin-dependent diabetes patients: A long-term follow-up. Acta Ophthalmol Scand 2002;80:305–309.
11. Yonemura D, Aoki T, Tsuzuki K. Electroretinogram in diabetic retinopathy. Arch Ophthalmol 1962;68:19–24.
12. McCulloch DL, Marmor MF, Brigell MG, Hamilton R, Holder GE, Tzekov R, Bach M. ISCEV Standard for full-field clinical electroretinography (2015 update). Doc Ophthalmol 2014;130:1–12.
13. Marmor MF, Fulton AB, Holder GE, Miyake Y, Brigell M, Bach M, International Society for Clinical Electrophysiology of V. ISCEV Standard for full-field clinical electroretinography (2008 update). Doc Ophthalmol 2009;118:69–77.
14. Rosolen SG, Rigaudiere F, Le Gargasson JF, Chalier C, Rufiange M, Racine J, Joly S, Lachapelle P. Comparing the photopic ERG i-wave in different species. Vet Ophthalmol 2004;7:189–192.
15. Lyubarsky AL, Lem J, Chen J, Falsini B, Iannaccone A, Pugh EN, Jr. Functionally rodless mice: transgenic models for the investigation of cone function in retinal disease and therapy. Vision Res 2002;42:401–415.
16. Gilmour GS, Gaillard F, Watson J, Kuny S, Mema SC, Bonfield S, Stell WK, Sauve Y. The electroretinogram (ERG) of a diurnal cone-rich laboratory rodent, the Nile grass rat (Arvicanthis niloticus). Vision Res 2008;48:2723–2731.
17. Yang S, Luo X, Xiong G, So KF, Yang H, Xu Y. The electroretinogram of Mongolian gerbil (Meriones unguiculatus): comparison to mouse. Neurosci Lett 2015;589:7–12.
18. Carter-Dawson LD, LaVail MM. Rods and cones in the mouse retina. I. Structural analysis using light and electron microscopy. J Comp Neurol 1979;188:245–262.
19. Jeon CJ, Strettoi E, Masland RH. The major cell populations of the mouse retina. J Neurosci 1998;18:8936–8946.
20. Szel A, Rohlich P. Two cone types of rat retina detected by anti-visual pigment antibodies. Exp Eye Res 1992;55:47–52.
21. Matsui Y, Katsumi O, Sakaue H, Hirose T. Electroretinogram b/a wave ratio improvement in central retinal vein obstruction. Br J Ophthalmol 1994;78:191–198.
22. Wachtmeister L. Oscillatory potentials in the retina: what do they reveal. Prog Retin Eye Res. 1998;17:485–521.
23. Hancock HA, Kraft TW. Oscillatory potential analysis and ERGs of normal and diabetic rats. Invest Ophthalmol Vis Sci 2004;45:1002–1008.
24. Shirao Y, Kawasaki K. Electrical responses from diabetic retina. Prog Retin Eye Res. 1998;17:59–76.
25. Benoit J, Lachapelle P. Temporal relationship between ERG components and geniculate unit activity in rabbit. Vision Res 1990;30:797–806.
26. Lachapelle P, Little JM, Polomeno RC. The photopic electroretinogram in congenital stationary night blindness with myopia. Invest Ophthalmol Vis Sci 1983;24:442–450.
27. Wachtmeister L, Dowling JE. The oscillatory potentials of the mudpuppy retina. Invest Ophthalmol Vis Sci 1978;17:1176–1188.
28. Bui BV, Fortune B. Ganglion cell contributions to the rat full-field electroretinogram. J Physiol 2004;555:153–173.
29. Dong CJ, Agey P, and Hare WA. Origins of the electroretinogram oscillatory potentials in the rabbit retina. Vis Neurosci 2004;21:533–543.
30. Holopigian K, Seiple W, Lorenzo M, Carr R. A comparison of photopic and scotopic electroretinographic changes in early diabetic retinopathy. Invest Ophthalmol Vis Sci 1992;33:2773–2780.
31. Bresnick GH, Palta M. Oscillatory potential amplitudes. Relation to severity of diabetic retinopathy. Arch Ophthalmol 1987;105:929–933.
32. Sakai H, Tani Y, Shirasawa E, Shirao Y, Kawasaki K. Development of electroretinographic alterations in streptozotocin-induced diabetes in rats. Ophthalmic Res 1995;27:57–63.
33. Yoshida A, Kojima M, Ogasawara H, Ishiko S. Oscillatory potentials and permeability of the blood-retinal barrier in noninsulin-dependent diabetic patients without retinopathy. Ophthalmology 1991;98:1266–1271.
34. Bresnick GH, Palta M. Temporal aspects of the electroretinogram in diabetic retinopathy. Arch Ophthalmol 1987;105:660–664.
35. Gouras P, MacKay CJ. Growth in amplitude of the human cone electroretinogram with light adaptation. Invest Ophthalmol Vis Sci 1989;30:625–630.
36. Rousseau S, McKerral M, Lachapelle P. The i-wave: bridging flash and pattern electroretinography. Electroencephalogr Clin Neurophysiol Suppl 1996;46:165–171.
37. Colotto A, Falsini B, Salgarello T, Iarossi G, Galan ME, Scullica L. Photopic negative response of the human ERG: losses associated with glaucomatous damage. Invest Ophthalmol Vis Sci 2000;41:2205–2211.
38. Viswanathan S, Frishman LJ, Robson JG, Harwerth RS, Smith EL, 3rd. The photopic negative response of the macaque electroretinogram: reduction by experimental glaucoma. Invest Ophthalmol Vis Sci 1999;40:1124–1136.
39. Viswanathan S, Frishman LJ, Robson JG, Walters JW. The photopic negative response of the flash electroretinogram in primary open angle glaucoma. Invest Ophthalmol Vis Sci 2001;42:514–522.
40. Li B, Barnes GE, Holt WF. The decline of the photopic negative response (PhNR) in the rat after optic nerve transection. Doc Ophthalmol 2005;111:23–31.
41. Machida S, Raz-Prag D, Fariss RN, Sieving PA, Bush RA. Photopic ERG negative response from amacrine cell signaling in RCS rat retinal degeneration. Invest Ophthalmol Vis Sci 2008;49:442–452.
42. Mojumder DK, Sherry DM, Frishman LJ. Contribution of voltage-gated sodium channels to the b-wave of the mammalian flash electroretinogram. J Physiol 2008;586:2551–2580.
43. Machida S, Gotoh Y, Tanaka M, Tazawa Y. Predominant loss of the photopic negative response in central retinal artery occlusion. Am J Ophthalmol 2004;137:938–940.
44. Kondo M, Sieving PA Primate photopic sine-wave flicker ERG: vector modeling analysis of component origins using glutamate analogs. Invest Ophthalmol Vis Sci 2001;42:305–312.

45. Khan NW, Kondo M, Hiriyanna KT, Jamison JA, Bush RA, Sieving PA. Primate Retinal Signaling Pathways: Suppressing ON-Pathway Activity in Monkey With Glutamate Analogues Mimics Human CSNB1-NYX Genetic Night Blindness. J Neurophysiol 2005;93:481–492.
46. Bush RA, Sieving PA. Inner retinal contributions to the primate photopic fast flicker electroretinogram. J Opt Soc Am A Opt Image Sci Vis 1996;13:557–565.
47. Krishna VR, Alexander KR, Peachey NS. Temporal properties of the mouse cone electroretinogram. J Neurophysiol 2002;87:42–48.
48. Qian H, Shah MR, Alexander KR, Ripps H. Two distinct processes are evident in rat cone flicker ERG responses at low and high temporal frequencies. Exp Eye Res 2008;87:71–75.
49. Viswanathan S, Frishman LJ, Robson JG. Inner-retinal contributions to the photopic sinusoidal flicker electroretinogram of macaques. Macaque photopic sinusoidal flicker ERG. Doc Ophthalmol 2002;105:223–242.
50. Alexander KR, Raghuram A, McAnany JJ. Comparison of spectral measures of period doubling in the cone flicker electroretinogram. Doc Ophthalmol 2008;117:197–203.
51. Horn FK, Gottschalk K, Mardin CY, Pangeni G, Junemann AG, Kremers J. On and off responses of the photopic fullfield ERG in normal subjects and glaucoma patients. Doc Ophthalmol 2011;122:53–62.
52. Naarendorp F, Williams GE. The d-wave of the rod electroretinogram of rat originates in the cone pathway. Vis Neurosci 1999;16:91–105.
53. Stockton RA, Slaughter MM. B-wave of the electroretinogram. A reflection of ON bipolar cell activity. J Gen Physiol 1989;93:101–122.